2013

Supplemental Data for Science 2013 Corder et al. Constitutive mu-opioid receptor activity leads to long-term endogenous analgesia and dependence

Renee R. Donahue, *University of Kentucky*

Supplementary Materials for

Constitutive μ-Opioid Receptor Activity Leads to Long-Term Endogenous Analgesia and Dependence

G. Corder, S. Doolen, R. R. Donahue, M. K. Winter, B. L. Jutras, Y. He, X. Hu, J. S. Wieskopf, J. S. Mogil, D. R. Storm, Z. J. Wang, K. E. McCarson, B. K. Taylor*

*Corresponding author. E-mail: brad.taylor@uky.edu

Published 20 September 2013, *Science* **341**, 1394 (2013)
DOI: 10.1126/science.1239403

This PDF file includes

Materials and Methods

Mice

At the beginning of all experiments the subjects were naïve, adult (6-10 weeks for behavioral and biochemical studies; 3-4 weeks for Ca^{2+} imagining studies), male C57BL/6, *AC1*$^{-/-}$, or littermate *AC1*$^{+/+}$ wild-type controls. All procedures were approved by the Institutional Animal Care and Use Committee at the University of Kentucky in accordance with American Veterinary Medical Association guidelines.

AC1$^{-/-}$ mice and *AC1*$^{+/+}$ mice, bred fully congenic onto a C57BL/6 background, were provided by the Storm Lab (Washington University, Seattle, WA, USA). Lines were maintained using heterozygote breeding and the genotype was confirmed by a tail-snip PCR.

Mice were housed in plastic cages (bedding and enrichment) of 4 same-sex littermates in a temperature controlled environment (14 hr: 10 hr light-dark cycle; lights on at 7:00 am) with *ad libitum* access to food and water. Upon arrival to the University of Kentucky Division of Laboratory Animal Resources, mice were habituated to the colony housing room for 1 week prior to any experimentation.

Complete Freund's Adjuvant (CFA) model of inflammatory pain.

Immediately following baseline assessment of mechanical thresholds, mice were lightly restrained and injected with CFA (5µl, non-diluted) into the intraplantar surface (ventral-medial) of the left hindpaw. Sham injuries consisted of a saline injection which controlled

for needle puncture and subcutaneous injectate, (5µl, 0.9%). To assess the development of tissue edema, we recorded the dorsal-ventral thickness of the injured paw with a fine digital caliper.

Plantar incision model of post-operative pain.

Mice were anesthetized with isoflurane anesthesia (1.5-2%) and the surface of the left hindpaw was wiped with antiseptic and alcohol. Using a #11 scalpel blade, an incision was begun 3 mm from the proximal edge of the heel, and extended 7 mm towards the digits (*23*). The underlying muscle was incised longitudinally. The skin was closed with two nylon 6-0 sutures and antibiotic ointment was applied. Sham animals underwent the same procedure without incision of the underlying muscle. Sutures were removed on Post-Operative Day 10.

Mouse (*in vivo*) drug administration

For subcutaneous injections (200 µl), unanaesthetized mice were lightly restrained and injected with a 27 G needle under the skin of the back, above the lumbar region. For intrathecal injections (5 µl), unanaesthetized mice were lightly restrained and a 30 G needle attached to a Hamilton microsyringe was inserted between the L5/L6 vertebrae and then punctured through the dura (confirmation by presence of reflexive tail flick) as previously described (*52*). For intraperitoneal injections unanaesthetized mice were lightly restrained and a 27 G needle was inserted through the abdominal wall into the peritoneal space and drugs were administered in a 200 µl volume. For chronic drug infusion, we implanted subcutaneous osmotic mini-pumps (0.25µl/hr for 14 d). Pumps

were primed in 37 °C saline for 48 hr prior to surgical implantation according to the manufacturer's instructions. Under isoflurane anesthesia (5% induction followed by 1.5-2.0% maintenance), a subcutaneous pocket was created above the lumbar region of the spinal column with a 1 cm skin incision above the scapulae, followed by blunt dissection of the skin from the connective tissues with blunt tipped scissors. The pump was then inserted with the flow moderator facing caudally, which rested just above the lumbar region of the spinal column. The skin incision was then sutured closed and wiped with Betadine. The pump was removed after 14d under anesthesia, followed by sterile wound closure and wiped with Betadine.

Drug dosing

The following drugs and doses were used for *in vivo* experiments: naltrexone HCl (NTX, gift of the NIDA Drug Supply Program; subcutaneous: 0.003 – 10.0 mg / kg / body weight, dissolved in 200 µl saline; intrathecal: 1µg in 5µl saline), naltrexone methobromide (NMB, gift of the NIDA Drug Supply Program; subcutaneous: 3 mg/kg in 200 µl saline; intrathecal: 0.3 µg in 5µl saline), naloxone (intraperitoneal: 3 mg/kg in 200 µl saline), Phe-Cys-Tyr-Trp-Orn-Thr-Pen-Thr-NH_2 (CTOP; intrathecal: 100 ng in 5µl saline), pertussis toxin (intrathecal: 0.5 µg in 5µl water), 6β-naltrexol hydrate (intrathecal: 10 µg in 5µl 1% DMSO), β-funaltrexamine HCl (intrathecal: 2.5 µg in 5µl water), (+)-MK-801 maleate (intrathecal: 1 µg in 5µl water; a dose of MK-801 devoid of overt motor effects), NB001 (intrathecal: 2.5 µg in 5µl water), N-Methyl-D-aspartic acid (NMDA; intrathecal: 30 pmol in 5µl water), forskolin (intrathecal:1.5 µg in 5µl 1% DMSO), and [D-Ala^2, N-Me-Phe^4, Gly^5-ol]-Enkephalin (DAMGO; intrathecal:10-30 pmol in 5 µl saline).

Mechanical hyperalgesia testing

All testing was begun between 10:00 am and noon in a temperature- and light-controlled room. Mice were acclimated for 30 - 60 min in the testing environment within a rectangular plastic box (15x4x4 cm; 3 white opaque walls and 1 clear wall) on a raised metal mesh platform. Baseline testing was conducted prior to and after injury, and at various time points after drug injection (as indicated in the figures). To evaluate mechanical hypersensitivity (hyperalgesia) we used a logarithmically increasing set of 8 von Frey filaments (Stoelting, Illinois), ranging in gram force from 0.007 to 6.0 g. These were applied perpendicular to the ventral-medial hindpaw surface with sufficient force to cause a slight bending of the filament. A positive response was characterized as a rapid withdrawal of the paw away from the stimulus fiber within 4 s. Using the up-down statistical method (*53*), the 50% withdrawal mechanical threshold scores were calculated for each mouse and then averaged across the experimental groups.

Conditioned Place Preference

The CPP apparatus consists of 3 Plexiglas chambers separated by manual doors. A center chamber (6 1/4‘‘W X 8 1/8’’ D X 13 1/8‘‘ H) connects the 2 end chambers, which are identical in size (10 3/8’’ W X 8 1/8‘‘ D X 13 1/8’’ H) but can be distinguished by texture of floor (rough versus smooth) and wall pattern (vertical versus horizontal stripes). Movement of mice and time spent in each chamber were monitored by 4 X 16 photobeam arrays and automatically recorded in CPP software.

Preconditioning was performed 18 d after CFA injury across 3 days (days 1-3) for 30 min each day when mice were exposed to the environment with full access to all chambers. On day 3, a preconditioning bias test was performed to determine whether a preexisting chamber bias existed. In this test, mice were placed into the middle chamber and allowed to explore the open field with access to all chambers for 15 min. Data were collected and analyzed for duration spent in each chamber. Animals spending more than 80% or less than 20% of the total time in an end chamber were eliminated from further testing.

We used a single conditioning protocol. On day 4 (21 d after CFA), mice first received naloxone (i.p.) + saline (i.t.) paired with a randomly chosen chamber in the morning. Four hr later, naloxone (i.p.) + lidocaine (0.04% i.t.) was paired with the other chamber in the afternoon. During conditioning, mice remained in the paired chamber, without access to other chambers, for 15 min immediately following saline or drug injection. Naloxone was used for its relatively short half-life. As with subcutaneous naltrexone (3 mg/kg), intraperitoneal naloxone (3 mg/kg) rapidly reinstated mechanical hyperalgesia in a repeatable manner (fig. S13). Naloxone-induced hyperalgesia resolved within 4 hr, ensuring no residual effects at the second conditioning session.

On the test day, 20 hr after the afternoon pairing (22 d after CFA), mice were placed in the middle chamber of the CPP box with all doors open, allowing free access to all chambers. Movement and duration of time spent in each chamber were recorded for 15 min for analysis of chamber preference.

Spontaneous nocifensive behavior

Following intrathecal injection of NMDA or forskolin, we recorded (15 min) the duration of nocifensive behavior, defined as caudally-directed scratching, licking or biting of the limbs, tail and trunk (*44*). Time spent on genital licking or grooming above the trunk mid-line was not scored. The number of spontaneous paw lifts/flinches was quantified separately.

Facial grimacing

On each testing day, mice were placed individually into Plexiglas cubicles (9 x 5 x 5 cm high) with clear walls and a wire mesh floor. Fifteen min later, cameras directed at the front and back of the cubicle were turned on for 30 min. One clear facial image was taken for each 3-min interval using Rodent Face Finder® software (*54*). The images were randomized and scored for facial grimacing using the Mouse Grimace Scale as previously described previously (*55*).

pERK stimulation studies

A light-touch stimulation protocol was used as previously described (*56*). Briefly, mice were injected with vehicle or drug, and then 30 min later were anesthetized with isoflurane (1.5 %). A cotton-tip was gently stroked across the plantar surface of the ipsilateral hindpaw, once every 5 s for 5 min. After an additional 5 min, mice were transcardially perfused with 10% buffered formalin and the lumbar spinal cord was dissected. Control mice that did not receive the light-touch stimulation still underwent isoflurane anesthesia.

Histology and Immunohistochemistry

Mice were deeply anesthetized with isoflurane or an intraperitoneal overdose injection of Fatal Plus (86 mg/kg). Mice were then perfused with ice-cold PBS/heparin followed by ice-cold 10% buffered formalin. Spinal cords (L3 -L5) were postfixed in 10% formalin, cryoprotected in 30% sucrose, and sectioned at 30 μm on a sliding microtome.

Free-floating spinal cord sections were washed in 0.1M phosphate buffer, blocked in 3% normal goat serum containing 0.3% Triton-X, and incubated overnight in primary antibodies ((rabbit phospho-ERK1/2 antiserum (1:500, Cell Signaling), mouse NeuN-Alexa488 (1:200, Millipore), rat GFAP (1:5,000, Invitrogen), and rat CD11b (1:5,000, AbD Serotec). Sections were washed and incubated in Alexa 568 or 488-conjugated goat anti-rabbit antibody (1:700; Invitrogen)) for 2 hr at room temperature, serial washed, slide mounted, and cover-slipped with ProLong Gold + DAPI counterstain. Images were captured using conventional or confocal fluorescence microscopy.

For pERK quantification, 5 spinal sections, separated by at least 120 μm, were randomly selected from each mouse and the number of pERK+ profiles were counted by a blinded observer and binned by Rexed lamina (I-II and III-V).

cAMP ELISA assay

For *in vivo* detection of intracellular cAMP levels, lumbar spinal cords were rapidly dissected 30 min after intrathecal injection. L3-L5 segments were quickly blocked, frozen on dry ice, and stored at -80 ºC for later use. cAMP measurements were performed using

a direct cAMP enzyme immunoassay according to the manufacturer's protocol (non-acetylated protocol with sensitivity = 0.39 pmol/ml; Enzo Life).

We utilized entire lumbar spinal cord section (dorsal and ventral) for the following reasons: 1) it was necessary to use the dorsal and ventral aspects to achieve sufficient sample (protein) quantities to run the cAMP ELISA in duplicate as well as to run a concurrent Bradford protein assay in duplicate for each spinal cord sample; 2) only dorsal horn neurons exhibited increased pERK expression, suggesting that the latent central sensitization processes exist in this region; and 3) The large majority of MOR expression is in the dorsal horn as well (*57*). Therefore, we believe that changes in cAMP reflect events in the dorsal horn and not the ventral horn.

GTPγS^{35} binding assay

The lumbar enlargement of the spinal cord was removed by hydrostatic pressure ejection and snap-frozen in methyl butane. 25 μm thick sections were cut and mounted on positively charged glass slides. All sections were treated identically. Therefore, any residual opioid content (as well as other conditions) was identical between the sections used for basal determinations or those incubated with or without β-funaltrexamine. Incubation in buffer for a total of 25 min is sufficient to wash out any opioid peptides or other agonists in the extracellular space before incubation with GTPγS^{35}. Sections were equilibrated in assay buffer (3 mM MgCl2, 100 mM NaCl, 0.2 mm EDTA, and 50mM Tris, pH 7.4) for 10 min and then in 1 mM (β-FNA studies) or 2 mM (DAMGO studies) GDP for 15 min both at room temperature. Agonist-stimulated binding was then

performed with 1 mM or 2 mM GDP (β-FNA or DAMGO, respectively) and 0.1 nM GTPγS^{35} and one of five serial dilutions ranging from 33 nM to 33 μM DAMGO or 100 nM to 10 μM β-FNA in water treated with a peptidase inhibitor cocktail containing 0.17 mg/ml bacitracin, 17 μg/ml leupeptin, 17 μg/ml chymostatin, and 0.85 mg/ml bovine serum albumin. Drug was omitted and replaced with either peptidase-treated water for basal determinations or 10 μM unlabeled GTPγS in water for nonspecific binding determinations. Slides were incubated in binding conditions at 24°C (room temp) for 2 hr and then rinsed twice with ice-cold 50 mM Tris-Cl, pH 7.4, for 2 min and twice with room temperature deionized water for 2 min. Slides were exposed to autoradiographic film for 8 hr. Densitometry of images was performed by measuring the mean number of pixels in lamina I of each left and right dorsal horn and subtracting the mean dorsal column background value. Percent stimulation over basal was calculated using the following equation:

$$\left[\frac{(dorsal\ horn - column) - nsb}{(dorsal\ horn\ basal - column\ basal) - nsb} \times 100\right] - 100$$

Concentration-response curves were generated using non-linear regression curve-fitting, and values for maximal stimulation (E_{max}) and half-maximal stimulating concentration (EC_{50}) were determined.

Calcium Imaging

Transverse spinal cord slices (300-450 μm) were incubated for 60 min at room temperature with Fura-2 AM (10 μM) and pluronic acid (0.1%) in oxygenated aCSF containing (in mM): NaCl 127, KCl 1.8, KH_2PO_4 1.2, $CaCl_2$ 2.4, $MgSO_4$ 1.3, $NaHCO_3$ 26, glucose 15. This was followed by a 20 min de-esterification period in normal aCSF.

Slices were perfused at 1–2 ml/min with normal aCSF in an RC-25 recording chamber mounted on a Nikon FN-1 upright microscope fitted with a 79000 ET FURA2 Hybrid filter set and an HQ2 camera. Relative intracellular Ca^{2+} levels were determined by measuring the change in ratio of fluorescence emission at 510 nm in response to excitation at 340 and 380 nm (200 ms exposure). Paired images were collected at 1–1.5 seconds/frame. Relative changes in Ca^{2+} levels were evaluated using Nikon Elements software by creating a region of interest over the cell body and calculating the peak change in ratio. The peak magnitude of Ca^{2+} transient was expressed as difference in exposure to exogenous glutamate compared to baseline before glutamate. The criteria for a Ca^{2+} response required at least a 10% increase above the baseline ratio. Ca^{2+} transients were in response to a 10 s exposure to 0.3 mM glutamate. In opioid receptor antagonist studies, the slice was perfused with antagonist for 15 min prior to and during glutamate stimulation. Only cells that displayed a consistent control response to 1 mM glutamate at the beginning and end of the experiment (showing a less than 40% decrease in glutamate-evoked Ca^{2+} transients) were included in this study.

Statistics

Data were analyzed using one-way or two-way ANOVA, as indicated in the main text or figure captions, followed by Bonferroni post-hoc tests or Student's *t* tests as appropriate. For dose-response hyperalgesia studies the best-fit line was generated following non-linear regression analysis based on the Maximum Possible Effect (MPE) for each mouse; calculated as: MPE = [(drug induced threshold – basal threshold) / basal threshold] x 100; For GTPγS^{35} binding studies the best fit line was generated following non-linear regression analysis.

Supplementary Figures S1 to S13

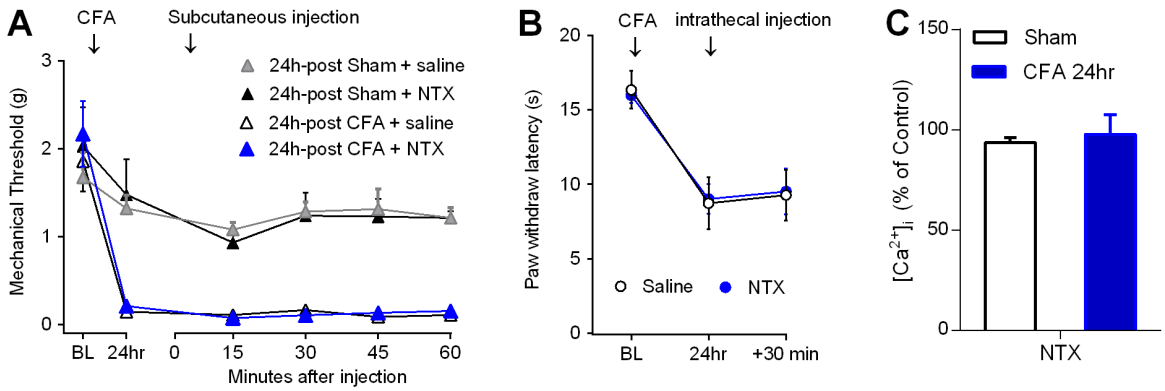

Fig. S1. NTX does not alter the induction phase of CFA-induced hyperalgesia or glutamate-evoked $[Ca^{2+}]_i$**.**

(A) 24 hr following intraplantar CFA (5 µl), a subcutaneous injection of NTX (3 mg/kg) did not increase mechanical hyperalgesia as measured by von Frey filaments (n = 5-6)

(B) 24 hr following intraplantar CFA, an intrathecal injection of NTX (1 µg) did not increase heat hyperalgesia as measured with a radiant heat paw-withdrawal test (n = 10 per group)

(C) In spinal cord slices collected 24 hr after Sham (n = 2 mice, 1-2 slices each) or CFA (n = 4 mice, 1-2 slices each), NTX perfusion (10 µM) did not change lamina II $[Ca^{2+}]_i$ that was evoked by brief (10s) glutamate perfusion.

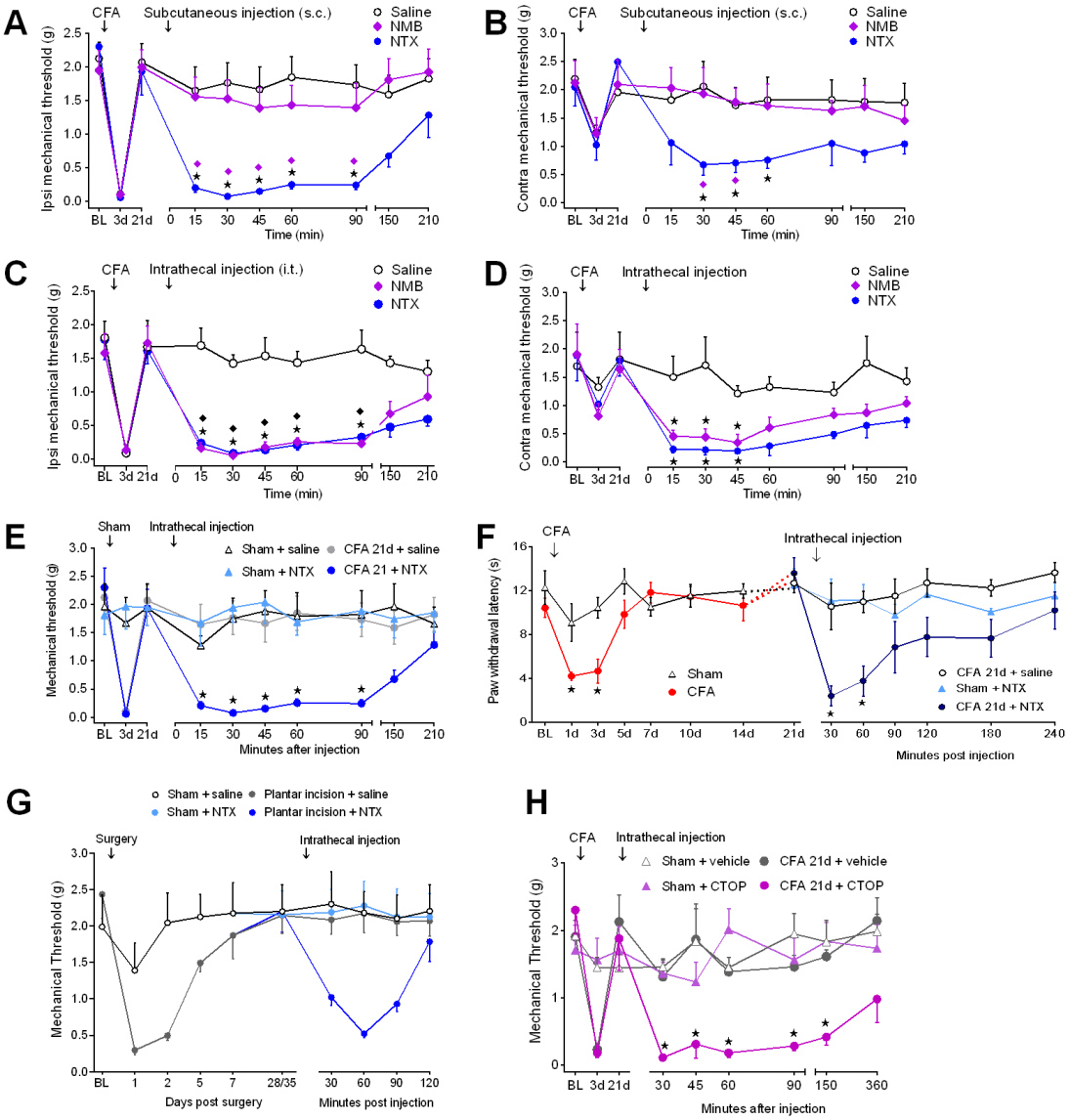

Fig. S2. Inflammation increases MOR signaling that tonically suppresses inflammatory pain: Time course of drug action for data of Figure 1.

(A, B, refers to Panel E of Fig 1**)** Effect of s.c. NTX or NMB on mechanical hyperalgesia in CFA-21d mice at **(A)** ipsilateral paw ($F_{2,19} = 6.5$, $P < 0.01$; n = 7-10) and **(B)** contralateral paw ($F_{2,16} = 3.9$, $P < 0.05$; n = 7-10). **(C,D,** refers to Panel F**)** Effect of i.t. NTX or NMB on mechanical hyperalgesia in CFA-21d mice at **(C)** ipsilateral paw ($F_{2,63} = 25$, $P < 0.0001$; n = 7 per group) or **(D)** contralateral paw ($F_{2,9} = 23.2$, $P < 0.0005$; n = 4 per group). **(E)** Effect of i.t. NTX in Sham and CFA-21d mice. Panel G ($F_{3,21} = 7.8$, $P = 0.0011$, 2-way ANOVA of all 4 groups; $F_{1,8} = 0.08$, $P = 0.79$, 2-way ANOVA of the 2 sham groups; n = 5-8). **(F)** Effect of i.t. NTX on heat hyperalgesia in CFA-21d mice. Panel H ($F_{2,19} = 6.5$, $P < 0.01$; n = 5-10. **(G)** Effect of i.t. NTX on mechanical hyperalgesia in Paw incision-21d mice. Panel J ($F_{3,30} = 5.4$, $P < 0.005$; n = 6-11. **(H)** Effect of i.t. CTOP on mechanical hyperalgesia in CFA-21d mice. Panel O ($F_{3,20} = 9.8$, $P < 0.0005$; n = 5-7). Two-way ANOVA with Bonferonni post-hoc test. Only 21d baseline and post-drug time points were included for ANOVA statistical analysis. ★ $P < 0.05$. All data shown as mean ± s.e.m.

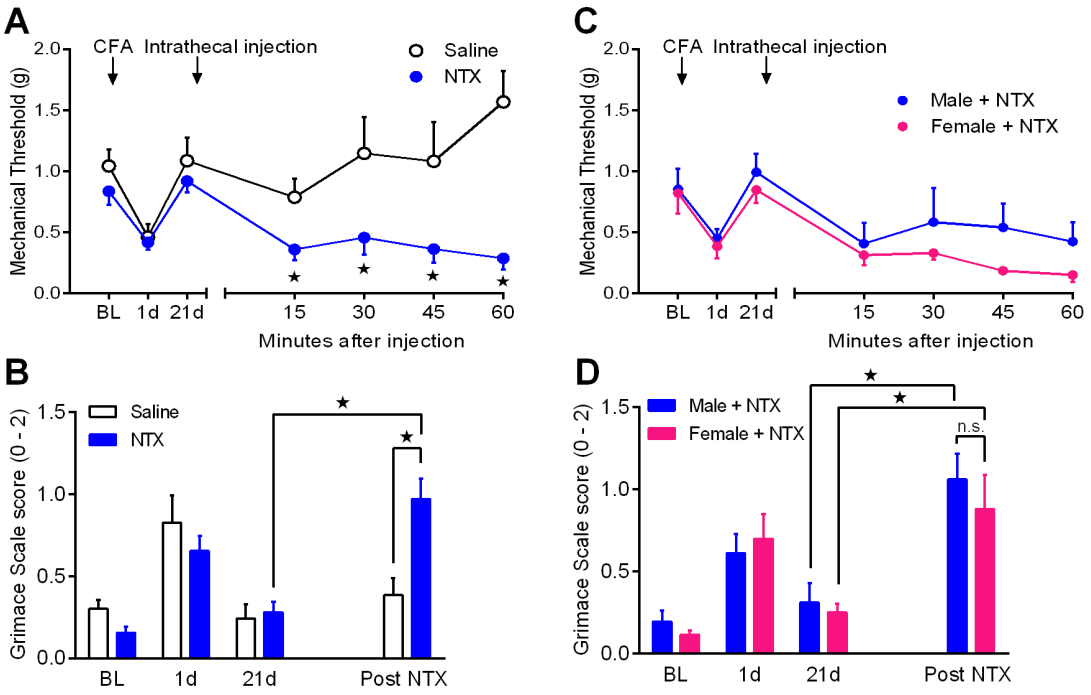

Fig. S3. NTX reinstatement of mechanical hyperalgesia and spontaneous pain in both sexes.

(A,B) Effect of intrathecal injection of saline or NTX on **(A)** von Frey threshold and **(B)** spontaneous pain measured by facial grimacing (Mouse Grimace Scale; mean MGS from 30-60 min post NTX) in CFA-21d mice (n = 4-8). **(C,D)** NTX group data from each sex are shown separately (n = 4 for each sex). In both sexes, significant Drug x Repeated Measures interaction were observed (von Frey: $F_{7,56} = 7.0$, $P < 0.005$; MGS: $F_{3,24} = 5.6$, $P = 0.005$); there were no main effects of or interactions with sex. ★$P < 0.05$. Error bars are s.e.m. 'Post-NTX' data of Panel B are also shown as Figure 1I.

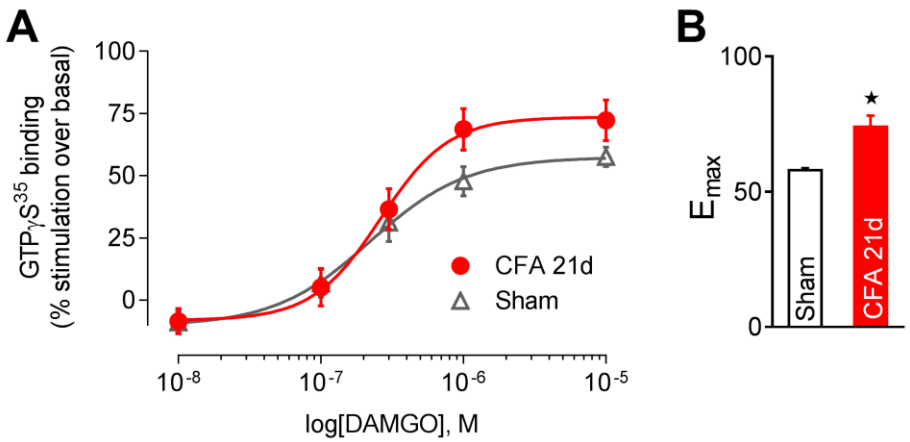

Fig. S4. DAMGO-stimulated GTPγS^{35} binding in the contralateral dorsal horn is increased in CFA-21d mice.

(A) Dose-response effects of DAMGO on GTPγS^{35} binding compared to basal binding in Sham and CFA-21d lumbar spinal cord slices; **(B)** Maximal physiological effect, E_{max}. (n = 7-9). Best-fit line calculated by non-linear regression. ★ $P < 0.05$, Student's *t* test. All data shown as mean ± s.e.m.

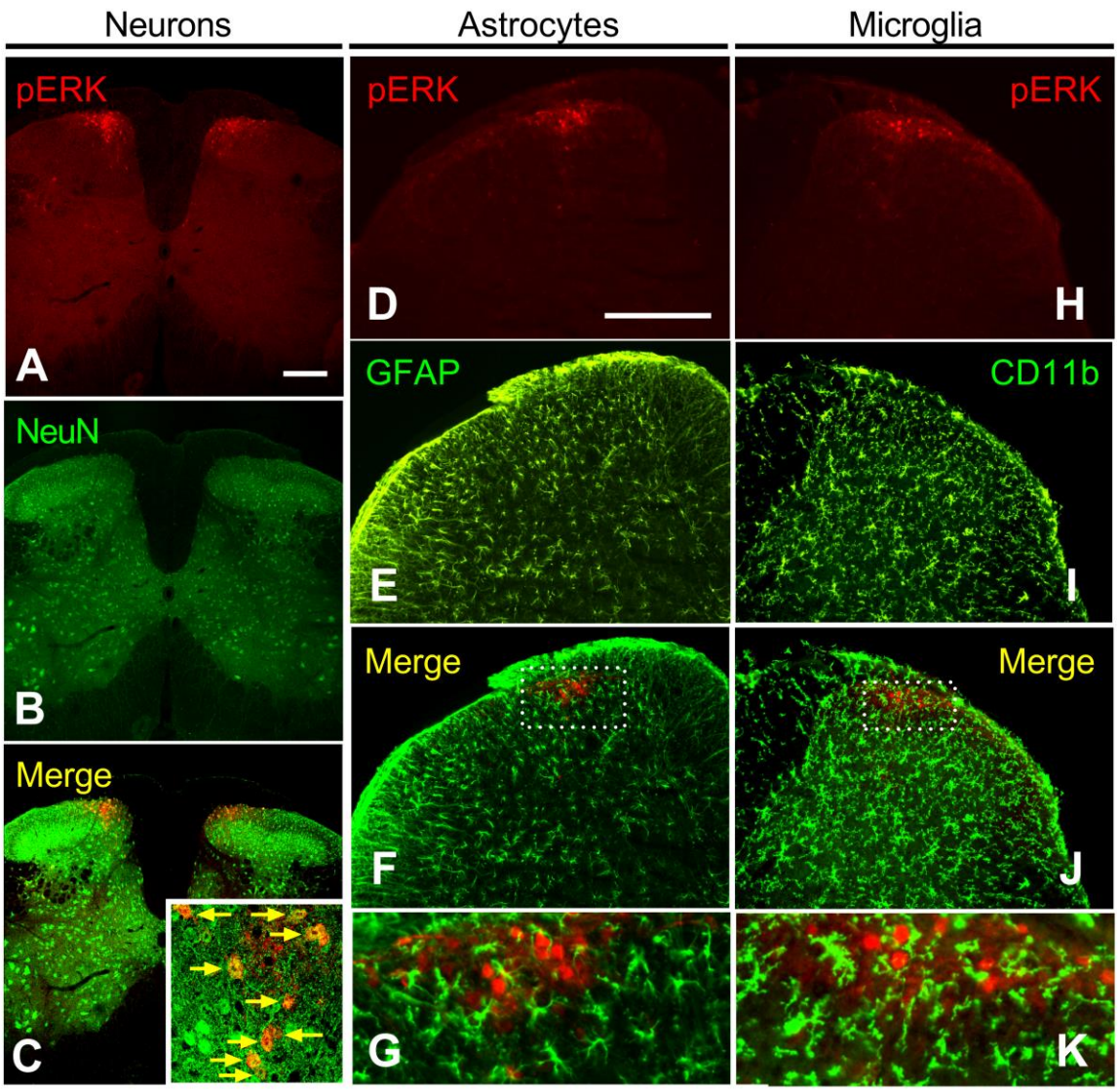

Fig. S5. Light-touch evoked spinal pERK is co-localized within neurons but not astrocytes or microglia.

Representative spinal cord sections (30 μm) from CFA-21d mice given intrathecal naltrexone (1 μg) and an ipsilateral light-touch paw stimulation (see Supplementary Methods) were co-stained for phosphorylated extracellular regulated kinase (rabbit, 1:700 Cell Signaling) and either **(A-C)** NeuN::Alexa-488 (rat, 1:200, Millipore; confocal images taken at 5x; *inset:* 40x), **(D-G)** GFAP (rat, 1:5000, Invitrogen; light microscope images taken at 10x for panels D-F and 40x for panel G) or **(H-K)** CD11b (rat, 1:5000, AbD Serotec; light microscope images taken at 10x for panels H-J and 40x for panel K). All scale bars are 200 μm. Panels A-C are from the same spinal cord slice shown in Fig. 1T-W. See Cover of the Sept 20th, 2013 issue for a 63X image from a section stained as in **(C)**.

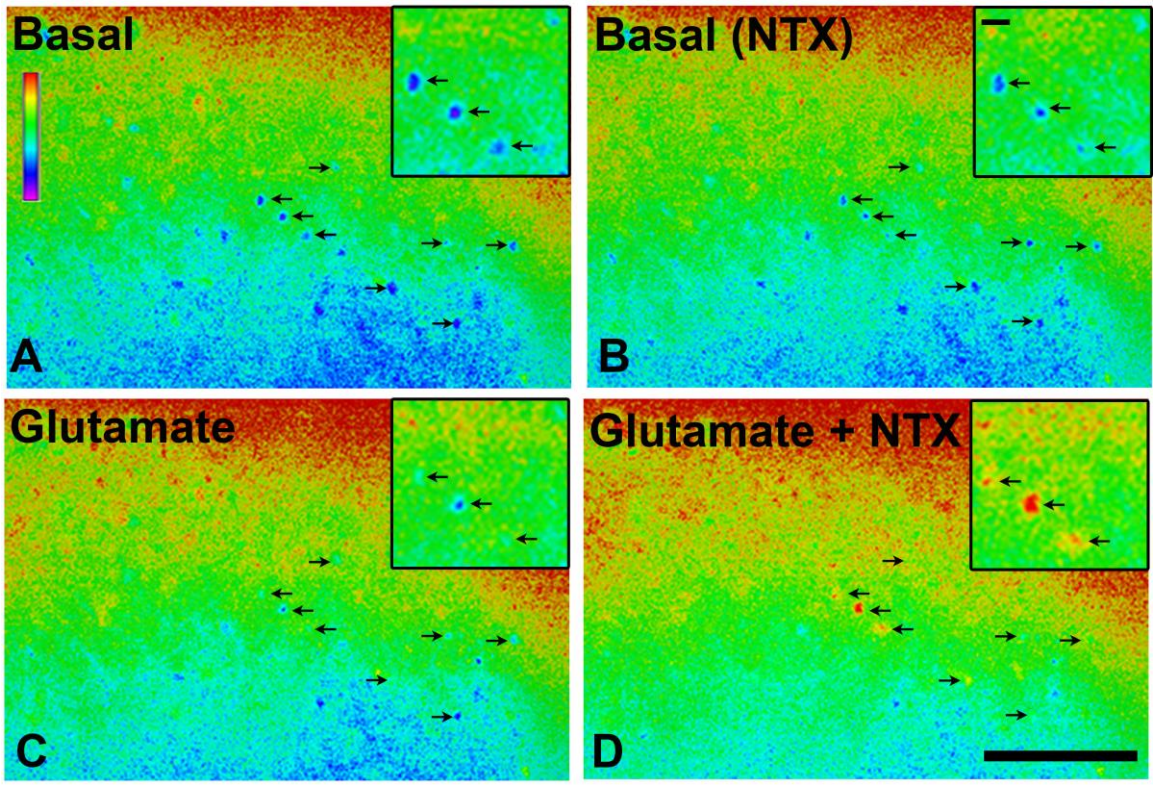

Fig. S6. NTX potentiates glutamate-evoked intracellular calcium mobilization.

Representative ratiometric (Δ340/380 nm) image of $[Ca^{2+}]_i$ in lamina II dorsal horn neurons from a CFA-21d spinal cord slice. Cells responding to bath application of control perfusate (A), 10 µM naltrexone (B), 0.3mM glutamate (C), or glutamate + naltrexone 15 min prior to glutamate stimulation **(D)**. Arrows designate Fura-2 loaded, glutatmate-responsive cells. Color intensity correspond to $[Ca^{2+}]_i$ .Color ratio scale: Low = pink = 0.64, high = red = 0.82. Scale bar = 100 µm, inset scale bar = 10 µm. This image is the same slice as the F380nm image from Fig. 2C.

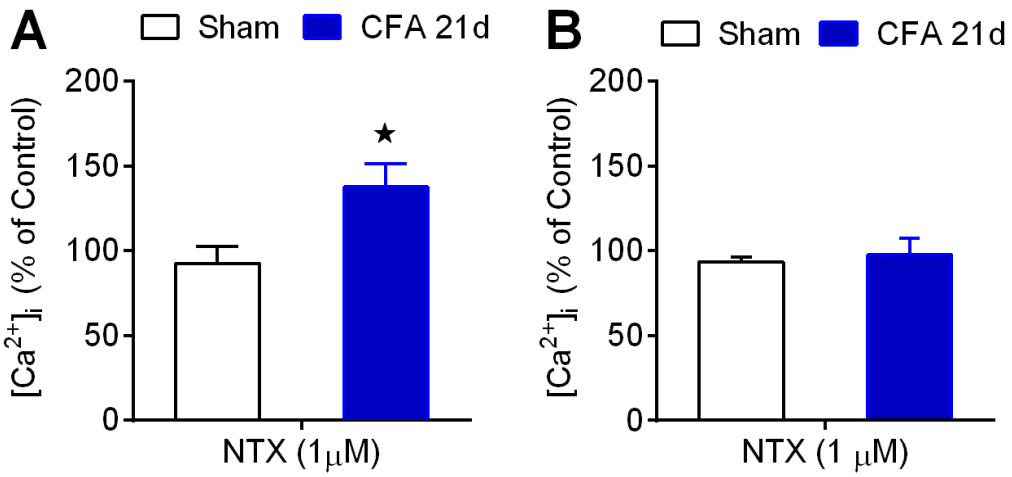

Fig. S7. Naltrexone increased glutamate-evoked $[Ca^{2+}]_i$ in lamina I cells at the side ipsilateral but not contralateral to inflammation.

(A) NTX (10 μM) perfusion increased glutamate-evoked $[Ca^{2+}]_i$ in lamina I cells from CFA-21d spinal cord slices (n = 5 mice, total of 9 slices) as compared to lamina I cells from sham slices (n = 4 mice, total of 6 slices). ★ $P = 0.0392$. **(B)** NTX-perfusion produced similar glutamate-evoked $[Ca^{2+}]_i$ in CFA-21d spinal cord slices (n = 4 mice, total of 6 slices) and sham slices (n = 2 mice, total of 4 slices) in contralateral lamina I-II cells.

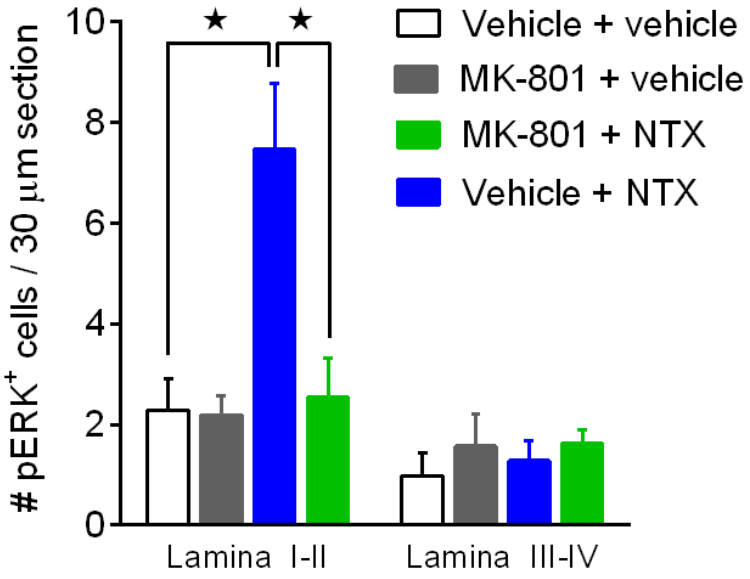

Fig. S8. NMDA-R signaling is necessary for contralateral pERK immunoreactivity during opioid receptor blockade.

Effect of intrathecal MK-801 (1µg) on NTX-induced (1µg) pERK expression in lamina I-II (left) or III-V (right), contralateral to light-touch stimulation of the left hindpaw (n = 6-10). ★ $P < 0.05$. Student's *t* test. All data shown as mean ± s.e.m.

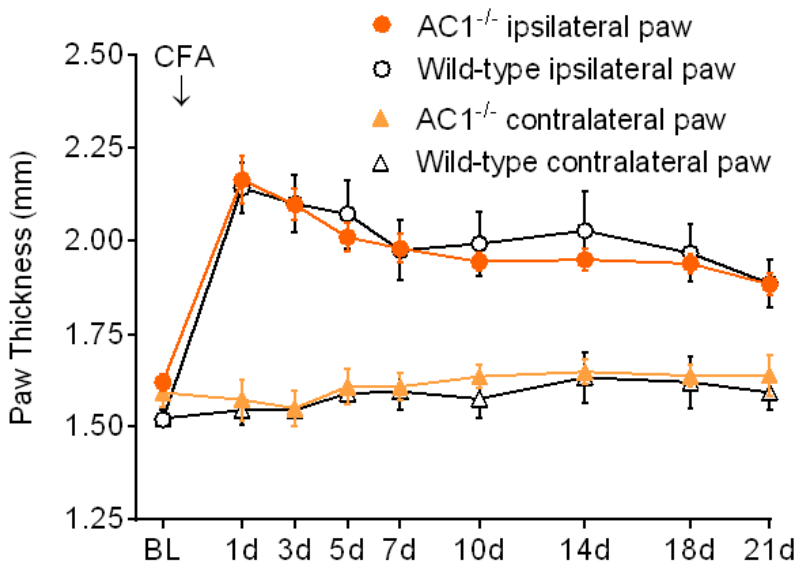

Fig. S9. AC1 gene deletion does not change the tissue edema induced by CFA.
Time course of CFA-induced edema in $AC1^{-/-}$ and littermate Wild-type ($AC1^{+/+}$) mice. The dorsal-ventral thickness of the ipsilateral and contralateral paws was measured by a fine-caliper before (baseline, BL) and after ipsilateral intraplantar CFA (5 µl) injection. (n = 5-9).

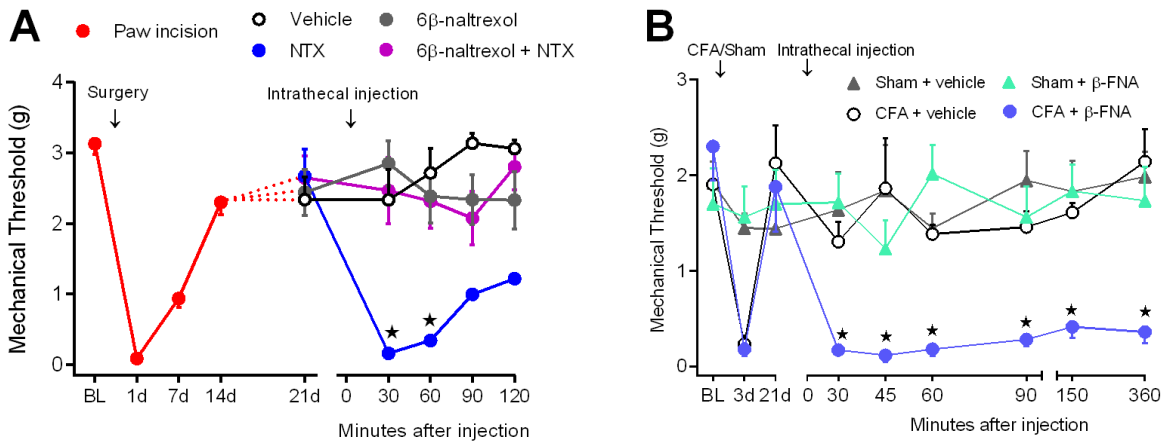

Fig. S10. Pharmacological time course data of panels D-E in Figure 3.

(A) Effect of intrathecal injection of 6β-naltrexol (10 μg) and/or NTX (1 μg) on mechanical hyperalgesia when administered 21 days after plantar paw incision surgery ($F_{3,21}$ = 18.1, P < 0.0001; n = 6-7, Panel D of Fig 3). **(B)** Effect of intrathecal β-funaltrexamine (2.5 μg) on mechanical hyperalgesia when administered 21 days after CFA ($F_{3,20}$ = 15.9, P < 0.0001; n = 5-7, Panel E). These data indicate that β-funaltrexamine can rapidly block MOR, in accordance with previous literature showing: 1) reversible binding to MOR within 30 min (*58*); 2) rapid precipitation of withdrawal behaviors during the opiate-dependent state (*59-61*). ★ P < 0.05. Two-way ANOVA with Bonferroni post-hoc test. Data are s.e.m.

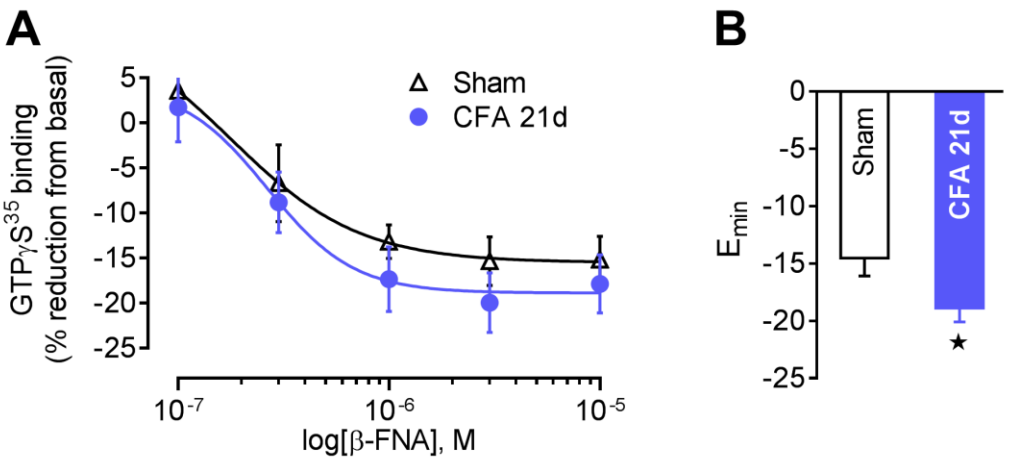

Fig. S11. β-funaltrexamine (β-FNA) decreases basal GTPγS^{35} binding in the contralateral dorsal horn.

(A) Dose-response effects of β-FNA on basal GTPγS^{35} binding in Sham and CFA-21d lumbar contralateral dorsal horns; **(B)** binding E_{min} averaged across dose of β-FNA. (*n* = 7-9). All data shown as mean ± s.e.m. ★ $P < 0.05$.

β-FNA effects on E_{max} and EC_{50}:
CFA-21d ipsilateral dorsal horn, E_{min} of -30.94 ± 0.74% and an EC_{50} of 0.55 ± 0.05 µM
CFA-21d contralateral dorsal horn, E_{min} of -18.89 ± 1.19% and an EC_{50} of 0.3 ± 0.07 µM
Sham ipsilateral dorsal horn, E_{min}: -15.44 ± 0.31%; EC_{50}: 0.23 ± 0.04 µM
Sham contralateral dorsal horn, E_{min}: -14.51 ± 1.57%; EC_{50}: 0.38 ± 0.11 µM.

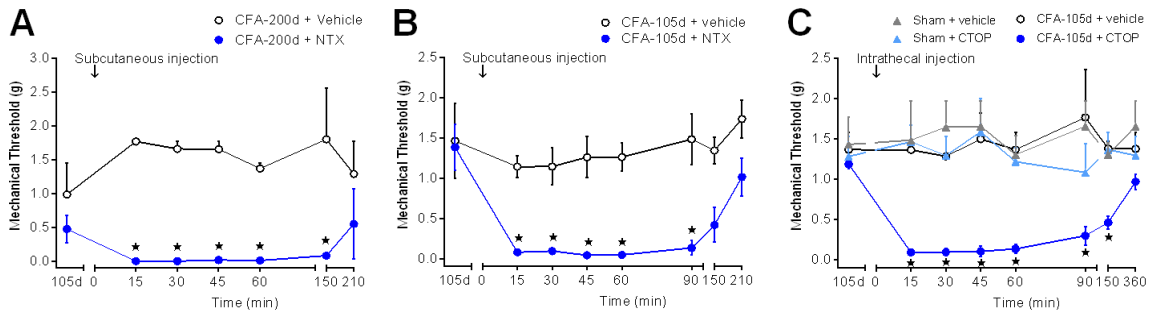

Fig. S12. Long-lasting spinal MOR activity.

(A) Effect of subcutaneous vehicle or NTX (3 mg/kg) on mechanical thresholds 200 d after CFA. These data indicate that opioid receptor-mediated anti-hyperalgesia lasts for months ($F_{1,2}$ = 9.4, P = 0.01; n = 2 per group). **(B)** Effect of a single subcutaneous injection of NTX (3 mg/kg, n = 11) or vehicle (n = 5) on mechanical thresholds 105d after CFA (Panel B: $F_{1,14}$ = 28.8, P < 0.0001. **(C)** Effect of a single intrathecal injection of CTOP (100 ng; Sham: n = 3; CFA-105d: 5) or vehicle (Sham: n = 3; CFA-105d: 3) ($F_{3,10}$ = 9.9, P < 0.005) on mechanical thresholds 105d after CFA. Prior to experimentation, mice only received CFA, and were never exposed to drugs, behavioral testing equipment, or the testing room.

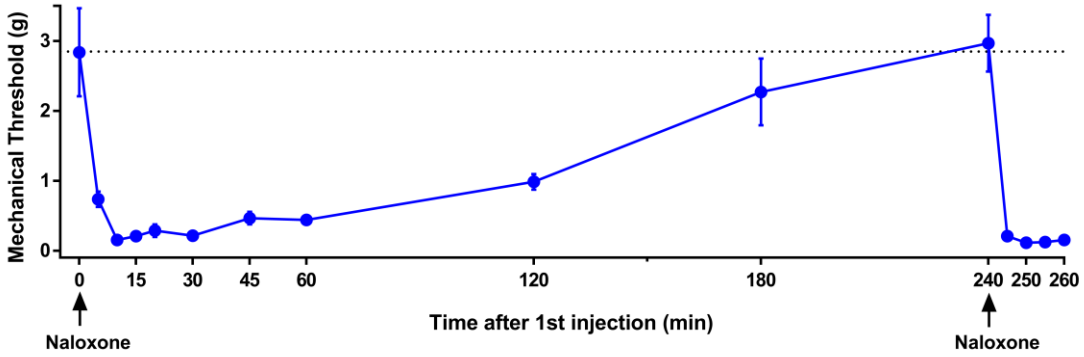

Fig. S13. Naloxone reinstates a relatively short-lasting mechanical hyperalgesia in the post-hyperalgesia state.

To mimic the conditions of the conditioned place preference studies of Fig 4A, we administered two sequential intraperitoneal injections of naloxone (3 mg/kg, 200 µl), 4 hr apart. The first naloxone injection produced a decrease in mechanical threshold at 5, 10, 15, 20, 30, 45, 60, and 120 min, which fully resolved within 4 hrs (relatively short compared to naltrexone). Hyperalgesia could again be reinstated with a second naloxone injection. (n = 4). Data shown as mean ± s.e.m.

Supplementary Notes

Supplementary Text S1

The induction phase of CFA-hyperalgesia (<24 hrs after injury) is dependent on spinal NMDA-R signaling, whereas the maintenance phase of hyperalgesia has NMDA-R-independent components. As illustrated in fig. S1A-C, NTX does not increase hyperalgesia or glutamate-evoked spinal $[Ca^{2+}]_i$ 24 hr after CFA, suggesting that the endogenous opioidergic system does not impinge on the induction of CFA-hyperalgesia. In contrast, as illustrated in Figure 1B, continuous infusion of NTX over the first 14d after CFA eliminated endogenous opioid analgesia, suggesting that the opioidergic system opposes the maintenance of CFA-hyperalgesia. Taken together, our data suggest that the cellular mechanisms of the induction and maintenance of latent hyperalgesia in our model are different.

Supplementary Text S2

Basal spinal cAMP levels were similar between shams and CFA-21d animals with MOR_{CA}. This could reflect a two-stage homeostatic process similar to that which occurs following chronic opiate administration. First, CFA might initiate an endogenous MOR-mediated decrease in cAMP. Second, a homeostatic up-regulation of AC would normalize cAMP levels back to baseline levels. Indeed, as occurs after chronic opioid administration, we demonstrated not only increased sensitivity to intrathecal forskolin, but also cAMP overshoot after administration of opioid receptor inverse agonists.

Supplementary Text S3

It remains an interesting question as to what mechanisms initiate and maintain constitutive signaling after inflammation. Chronic stimulation of MORs with repeated morphine administration can produce constitutive activity; this is enhanced by endogenously released enkephalins (*20*). Therefore, we believe that injury increases spinal opioid peptide release, which then facilitates the induction of MOR_{CA}. While we have no direct evidence of the molecular mechanisms driving the acquisition of MOR_{CA} in our model, we refer to the Extended Ternary Complex model of GPCR signaling (*32*). In this modeling paradigm, constitutive activity can be produced by lowering the energy barrier to generate the spontaneous formation of the receptor active state. This is referred to as a decrease in allosteric constant, and might be achieved through post-translation modification of MOR (e.g. hyper-phosphorylation) (*17*) or a reduction in the association of the receptor with a negative regulatory protein, such as β-arrestin2 (*37*).

Supplementary Text S4

A large body of evidence indicates that naltrexone can act as an inverse agonist while 6β-naltrexol is a neutral antagonist, particularly in the setting of chronic opiate exposure (*35, 37, 62*).

Supplementary Text S5

Repeated administration of opiates typically produce tolerance in rodents. We found that tonic MOR signaling lasted for months after CFA, without signs of endogenous tolerance (i.e. return of hyperalgesia). This might be explained by a bias of endogenous opioids that favors analgesia over analgesic tolerance mechanisms, such as β-arrestin2-mediated receptor internalization (*63*). Several pieces of evidence support this. First, CFA reduces morphine cross-tolerance (*64*). Second, β-arrestin2 KO mice exhibit increased morphine antinociception (*63*) and decreased tolerance (*65*) that rely on MOR constitutive activity (*37*). Third, the enkephalinase inhibitor, RB101, produces analgesia that does not undergo tolerance or cross-tolerance to morphine (*66*).

Supplementary Text S6

Naloxone can produce hyperalgesia in humans, indicating the presence of endogenous opioid analgesia (*67-69*). Furthermore, tonic pain causes the release of endogenous substances acting at MORs in the brain (*70*), and induces long-lasting activation of spinal MOR (*71*). Our data suggest that endogenous activation of MORs will initiate both analgesic signaling as well as a standard compensatory opponent-processes that can lead to a rebound effect when an inverse agonist is given (i.e. withdrawal symptoms). Indeed, anecdotal evidence supports the idea that endogenous opioidergic mechanisms lead to physical dependence in humans. For example, naltrexone can induce withdrawal-like symptoms including nausea and jitteriness (*72*).

Supplementary Text S7

Unilateral injuries often produce bilateral hyperalgesia, and the current data extends this to latent pain sensitization in CFA 21-day mice. NTX produced bilateral hyperalgesia and bilaterally increased stimulus-evoked pERK expression. Leading explanations for bilateral hyperalgesia include descending facilitatory fibers from the brainstem (*73, 74*) and reactive spinal astrocytes communicating through gap-junction networks (*56, 75*). We found evidence for bilateral expression of MOR_{CA}, namely contralateral increases in DAMGO-induced MOR-G-protein coupling and β-funaltrexamine-induced decreases in

basal MOR-G-protein coupling. We suggest that MOR_{CA} is intricately involved in the regulation of contralateral sensitization, and thus chronic pain phenotypes that display widespread hypersensitivity, such as fibromyalgia.

Supplementary Text S8

NTX-induced pain reinstatement (e.g. abrupt withdrawal from MOR_{CA} by an inverse agonist) could result from either: 1) disinhibition of tonically active primary afferent terminals: 2) disinhibition of AC1 superactivation in dorsal horn neurons; 3) potentiation of descending facilitatory signals from the brainstem; and/or 4) induction of *de novo* spinal NMDA-R-dependent withdrawal. While we have no direct evidence of withdrawal-induced *de novo* LTP, several of our data and other studies suggest this as a promising area of future investigation:

1) Exogenous opiate withdrawal in the spinal cord initiates *de novo* NMDA-R-dependent LTP (*12, 76*); 2) NMDA-R signaling and post-synaptic spinal neuron Ca^{2+} rise are required in the induction, rather than maintenance, of spinal LTP and hyperalgesia (*77, 78*); 3) AC1 is activated by NMDA-R-derived Ca^{2+} and is necessary for LTP induction (*30, 79, 80*); 4) Intrathecal NMDA (3 pmol) increased pain behaviors and spinal cAMP levels in CFA-21d mice compared to shams (Fig. 2H and 2I). This suggests that spinal NMDA-R–adenylyl cyclase signaling pathways are not occluded (saturated); and 5) Intrathecal MK-801alone did not increase mechanical threshold (Fig. 2D), decrease basal pERK expression (Fig. 2E), or decrease basal cAMP levels (Fig. 2G) when administered during the post-hyperalgesia state. And MK-801 perfusion did not reduce basal spinal intracellular calcium levels from CFA-21d slices (Fig 2C). These findings suggest that spinal NMDA-Rs are not active prior to NTX-induced withdrawal.

References

1. A. Latremoliere, C. J. Woolf, Central sensitization: A generator of pain hypersensitivity by central neural plasticity. *J. Pain* **10**, 895–926 (2009). doi:10.1016/j.jpain.2009.06.012 Medline

2. H. Ikeda, J. Stark, H. Fischer, M. Wagner, R. Drdla, T. Jäger, J. Sandkühler, Synaptic amplifier of inflammatory pain in the spinal dorsal horn. *Science* **312**, 1659–1662 (2006). doi:10.1126/science.1127233 Medline

3. R. Ruscheweyh, O. Wilder-Smith, R. Drdla, X. G. Liu, J. Sandkühler, Long-term potentiation in spinal nociceptive pathways as a novel target for pain therapy. *Mol. Pain* **7**, 20 (2011). doi:10.1186/1744-8069-7-20 Medline

4. G. W. Terman, C. L. Eastman, C. Chavkin, Mu opiates inhibit long-term potentiation induction in the spinal cord slice. *J. Neurophysiol.* **85**, 485–494 (2001). Medline

5. J. Benrath, C. Brechtel, E. Martin, J. Sandkühler, Low doses of fentanyl block central sensitization in the rat spinal cord in vivo. *Anesthesiology* **100**, 1545–1551 (2004). doi:10.1097/00000542-200406000-00030 Medline

6. R. Drdla-Schutting, J. Benrath, G. Wunderbaldinger, J. Sandkühler, Erasure of a spinal memory trace of pain by a brief, high-dose opioid administration. *Science* **335**, 235–238 (2012). doi:10.1126/science.1211726 Medline

7. A. I. Basbaum, H. L. Fields, Endogenous pain control systems: Brainstem spinal pathways and endorphin circuitry. *Annu. Rev. Neurosci.* **7**, 309–338 (1984). doi:10.1146/annurev.ne.07.030184.001521 Medline

8. M. H. Ossipov, G. O. Dussor, F. Porreca, Central modulation of pain. *J. Clin. Invest.* **120**, 3779–3787 (2010). doi:10.1172/JCI43766 Medline

9. M. J. Christie, Cellular neuroadaptations to chronic opioids: Tolerance, withdrawal and addiction. *Br. J. Pharmacol.* **154**, 384–396 (2008). doi:10.1038/bjp.2008.100 Medline

10. T. Avidor-Reiss, I. Nevo, D. Saya, M. Bayewitch, Z. Vogel, Opiate-induced adenylyl cyclase superactivation is isozyme-specific. *J. Biol. Chem.* **272**, 5040–5047 (1997). doi:10.1074/jbc.272.8.5040 Medline

11. S. B. Lane-Ladd, J. Pineda, V. A. Boundy, T. Pfeuffer, J. Krupinski, G. K. Aghajanian, E. J. Nestler, CREB (cAMP response element-binding protein) in the locus coeruleus: Biochemical, physiological, and behavioral evidence for a role in opiate dependence. *J. Neurosci.* **17**, 7890–7901 (1997). Medline

12. R. Drdla, M. Gassner, E. Gingl, J. Sandkühler, Induction of synaptic long-term potentiation after opioid withdrawal. *Science* **325**, 207–210 (2009). doi:10.1126/science.1171759 Medline

13. C. Heinl, R. Drdla-Schutting, D. N. Xanthos, J. Sandkühler, Distinct mechanisms underlying pronociceptive effects of opioids. *J. Neurosci.* **31**, 16748–16756 (2011). doi:10.1523/JNEUROSCI.3491-11.2011 Medline

14. E. J. Nestler, G. K. Aghajanian, Molecular and cellular basis of addiction. *Science* **278**, 58–63 (1997). doi:10.1126/science.278.5335.58 Medline

15. J. A. Kauer, R. C. Malenka, Synaptic plasticity and addiction. *Nat. Rev. Neurosci.* **8**, 844–858 (2007). doi:10.1038/nrn2234 Medline

16. M. S. Angst, J. D. Clark, Opioid-induced hyperalgesia: A qualitative systematic review. *Anesthesiology* **104**, 570–587 (2006). doi:10.1097/00000542-200603000-00025 Medline

17. Z. Wang, E. J. Bilsky, F. Porreca, W. Sadée, Constitutive mu opioid receptor activation as a regulatory mechanism underlying narcotic tolerance and dependence. *Life Sci.* **54**, PL339–PL350 (1994). doi:10.1016/0024-3205(94)90022-1 Medline

18. J. G. Liu, P. L. Prather, Chronic exposure to mu-opioid agonists produces constitutive activation of mu-opioid receptors in direct proportion to the efficacy of the agonist used for pretreatment. *Mol. Pharmacol.* **60**, 53–62 (2001). Medline

19. D. Wang, K. M. Raehal, E. T. Lin, J. J. Lowery, B. L. Kieffer, E. J. Bilsky, W. Sadée, Basal signaling activity of mu opioid receptor in mouse brain: Role in narcotic dependence. *J. Pharmacol. Exp. Ther.* **308**, 512–520 (2004). doi:10.1124/jpet.103.054049 Medline

20. J. R. Shoblock, N. T. Maidment, Constitutively active micro opioid receptors mediate the enhanced conditioned aversive effect of naloxone in morphine-dependent mice. *Neuropsychopharmacology* **31**, 171–177 (2006). Medline

21. F. J. Meye, R. van Zessen, M. P. Smidt, R. A. Adan, G. M. Ramakers, Morphine withdrawal enhances constitutive μ-opioid receptor activity in the ventral tegmental area. *J. Neurosci.* **32**, 16120–16128 (2012). doi:10.1523/JNEUROSCI.1572-12.2012 Medline

22. J. R. Shoblock, N. T. Maidment, Enkephalin release promotes homeostatic increases in constitutively active mu opioid receptors during morphine withdrawal. *Neuroscience* **149**, 642–649 (2007). doi:10.1016/j.neuroscience.2007.05.011 Medline

23. E. M. Pogatzki, S. N. Raja, A mouse model of incisional pain. *Anesthesiology* **99**, 1023–1027 (2003). doi:10.1097/00000542-200310000-00041 Medline

24. C. Luo, P. H. Seeburg, R. Sprengel, R. Kuner, Activity-dependent potentiation of calcium signals in spinal sensory networks in inflammatory pain states. *Pain* **140**, 358–367 (2008). doi:10.1016/j.pain.2008.09.008 Medline

25. S. Doolen, C. B. Blake, B. N. Smith, B. K. Taylor, Peripheral nerve injury increases glutamate-evoked calcium mobilization in adult spinal cord neurons. *Mol. Pain* **8**, 56 (2012). doi:10.1186/1744-8069-8-56 Medline

26. D. M. Chetkovich, J. D. Sweatt, NMDA receptor activation increases cyclic AMP in area CA1 of the hippocampus via calcium/calmodulin stimulation of adenylyl cyclase. *J. Neurochem.* **61**, 1933–1942 (1993). doi:10.1111/j.1471-4159.1993.tb09836.x Medline

27. V. Zachariou, R. Liu, Q. LaPlant, G. Xiao, W. Renthal, G. C. Chan, D. R. Storm, G. Aghajanian, E. J. Nestler, Distinct roles of adenylyl cyclases 1 and 8 in opiate dependence: Behavioral, electrophysiological, and molecular studies. *Biol. Psychiatry* **63**, 1013–1021 (2008). doi:10.1016/j.biopsych.2007.11.021 Medline

28. M. S. Mazei-Robison, E. J. Nestler, Opiate-induced molecular and cellular plasticity of ventral tegmental area and locus coeruleus catecholamine neurons. *Cold Spring Harb Perspect Med* **2**, a012070 (2012). doi:10.1101/cshperspect.a012070 Medline

29. F. Wei, C. S. Qiu, S. J. Kim, L. Muglia, J. W. Maas Jr., V. V. Pineda, H. M. Xu, Z. F. Chen, D. R. Storm, L. J. Muglia, M. Zhuo, Genetic elimination of behavioral sensitization in mice lacking calmodulin-stimulated adenylyl cyclases. *Neuron* **36**, 713–726 (2002). doi:10.1016/S0896-6273(02)01019-X Medline

30. H. Wang, H. Xu, L. J. Wu, S. S. Kim, T. Chen, K. Koga, G. Descalzi, B. Gong, K. I. Vadakkan, X. Zhang, B. K. Kaang, M. Zhuo, Identification of an adenylyl cyclase inhibitor for treating neuropathic and inflammatory pain. *Sci. Transl. Med.* **3**, 65ra3 (2011). doi:10.1126/scitranslmed.3001269 Medline

31. T. Kenakin, Inverse, protean, and ligand-selective agonism: Matters of receptor conformation. *FASEB J.* **15**, 598–611 (2001). doi:10.1096/fj.00-0438rev Medline

32. T. Kenakin, Principles: Receptor theory in pharmacology. *Trends Pharmacol. Sci.* **25**, 186–192 (2004). doi:10.1016/j.tips.2004.02.012 Medline

33. T. Costa, A. Herz, Antagonists with negative intrinsic activity at delta opioid receptors coupled to GTP-binding proteins. *Proc. Natl. Acad. Sci. U.S.A.* **86**, 7321–7325 (1989). doi:10.1073/pnas.86.19.7321 Medline

34. R. Seifert, K. Wenzel-Seifert, Constitutive activity of G-protein-coupled receptors: Cause of disease and common property of wild-type receptors. *Naunyn Schmiedebergs Arch. Pharmacol.* **366**, 381–416 (2002). doi:10.1007/s00210-002-0588-0 Medline

35. K. M. Raehal, J. J. Lowery, C. M. Bhamidipati, R. M. Paolino, J. R. Blair, D. Wang, W. Sadée, E. J. Bilsky, In vivo characterization of 6beta-naltrexol, an opioid ligand with less inverse agonist activity compared with naltrexone and naloxone in opioid-dependent mice. *J. Pharmacol. Exp. Ther.* **313**, 1150–1162 (2005). doi:10.1124/jpet.104.082966 Medline

36. W. Sadée, D. Wang, E. J. Bilsky, Basal opioid receptor activity, neutral antagonists, and therapeutic opportunities. *Life Sci.* **76**, 1427–1437 (2005). doi:10.1016/j.lfs.2004.10.024 Medline

37. H. Lam, M. Maga, A. Pradhan, C. J. Evans, N. T. Maidment, T. G. Hales, W. Walwyn, Analgesic tone conferred by constitutively active mu opioid receptors in mice lacking β-arrestin 2. *Mol. Pain* **7**, 24 (2011). doi:10.1186/1744-8069-7-24 Medline

38. J. G. Liu, M. B. Ruckle, P. L. Prather, Constitutively active mu-opioid receptors inhibit adenylyl cyclase activity in intact cells and activate G-proteins differently than the agonist [D-Ala2,N-MePhe4,Gly-ol5]enkephalin. *J. Biol. Chem.* **276**, 37779–37786 (2001). Medline

39. T. King, L. Vera-Portocarrero, T. Gutierrez, T. W. Vanderah, G. Dussor, J. Lai, H. L. Fields, F. Porreca, Unmasking the tonic-aversive state in neuropathic pain. *Nat. Neurosci.* **12**, 1364–1366 (2009). doi:10.1038/nn.2407 Medline

40. Y. He, X. Tian, X. Hu, F. Porreca, Z. J. Wang, Negative reinforcement reveals non-evoked ongoing pain in mice with tissue or nerve injury. *J. Pain* **13**, 598–607 (2012). doi:10.1016/j.jpain.2012.03.011 Medline

41. K. J. Sufka, Conditioned place preference paradigm: A novel approach for analgesic drug assessment against chronic pain. *Pain* **58**, 355–366 (1994). doi:10.1016/0304-3959(94)90130-9 Medline

42. G. F. Koob, R. Maldonado, L. Stinus, Neural substrates of opiate withdrawal. *Trends Neurosci.* **15**, 186–191 (1992). doi:10.1016/0166-2236(92)90171-4 Medline

43. B. Kest, C. A. Palmese, E. Hopkins, M. Adler, A. Juni, J. S. Mogil, Naloxone-precipitated withdrawal jumping in 11 inbred mouse strains: Evidence for common genetic mechanisms in acute and chronic morphine physical dependence. *Neuroscience* **115**, 463–469 (2002). doi:10.1016/S0306-4522(02)00458-X Medline

44. M. N. Asiedu, D. V. Tillu, O. K. Melemedjian, A. Shy, R. Sanoja, B. Bodell, S. Ghosh, F. Porreca, T. J. Price, Spinal protein kinase M ζ underlies the maintenance mechanism of persistent nociceptive sensitization. *J. Neurosci.* **31**, 6646–6653 (2011). doi:10.1523/JNEUROSCI.6286-10.2011 Medline

45. M. De Felice, M. H. Ossipov, R. Wang, G. Dussor, J. Lai, I. D. Meng, J. Chichorro, J. S. Andrews, S. Rakhit, S. Maddaford, D. Dodick, F. Porreca, Triptan-induced enhancement of neuronal nitric oxide synthase in trigeminal ganglion dural afferents underlies increased responsiveness to potential migraine triggers. *Brain* **133**, 2475–2488 (2010). doi:10.1093/brain/awq159 Medline

46. C. Rivat, E. Laboureyras, J. P. Laulin, C. Le Roy, P. Richebé, G. Simonnet, Non-nociceptive environmental stress induces hyperalgesia, not analgesia, in pain and opioid-experienced rats. *Neuropsychopharmacology* **32**, 2217–2228 (2007). doi:10.1038/sj.npp.1301340 Medline

47. M. Zhuo, Targeting neuronal adenylyl cyclase for the treatment of chronic pain. *Drug Discov. Today* **17**, 573–582 (2012). doi:10.1016/j.drudis.2012.01.009 Medline

48. S. Li, M. L. Lee, M. R. Bruchas, G. C. Chan, D. R. Storm, C. Chavkin, Calmodulin-stimulated adenylyl cyclase gene deletion affects morphine responses. *Mol. Pharmacol.* **70**, 1742–1749 (2006). doi:10.1124/mol.106.025783 Medline

49. H. C. Lu, W. C. She, D. T. Plas, P. E. Neumann, R. Janz, M. C. Crair, Adenylyl cyclase I regulates AMPA receptor trafficking during mouse cortical 'barrel' map development. *Nat. Neurosci.* **6**, 939–947 (2003). doi:10.1038/nn1106 Medline

50. H. Xu, L. J. Wu, H. Wang, X. Zhang, K. I. Vadakkan, S. S. Kim, H. W. Steenland, M. Zhuo, Presynaptic and postsynaptic amplifications of neuropathic pain in the anterior cingulate cortex. *J. Neurosci.* **28**, 7445–7453 (2008). doi:10.1523/JNEUROSCI.1812-08.2008 Medline

51. C. Rivat, J. P. Laulin, J. B. Corcuff, E. Célèrier, L. Pain, G. Simonnet, Fentanyl enhancement of carrageenan-induced long-lasting hyperalgesia in rats: Prevention by the *N*-methyl-D-aspartate receptor antagonist ketamine. *Anesthesiology* **96**, 381–391 (2002). doi:10.1097/00000542-200202000-00025 Medline

52. C. A. Fairbanks, Spinal delivery of analgesics in experimental models of pain and analgesia. *Adv. Drug Deliv. Rev.* **55**, 1007–1041 (2003). doi:10.1016/S0169-409X(03)00101-7 Medline

53. S. R. Chaplan, F. W. Bach, J. W. Pogrel, J. M. Chung, T. L. Yaksh, Quantitative assessment of tactile allodynia in the rat paw. *J. Neurosci. Methods* **53**, 55–63 (1994). doi:10.1016/0165-0270(94)90144-9 Medline

54. D. J. Langford, A. L. Bailey, M. L. Chanda, S. E. Clarke, T. E. Drummond, S. Echols, S. Glick, J. Ingrao, T. Klassen-Ross, M. L. Lacroix-Fralish, L. Matsumiya, R. E. Sorge, S. G. Sotocinal, J. M. Tabaka, D. Wong, A. M. van den Maagdenberg, M. D. Ferrari, K. D. Craig, J. S. Mogil, Coding of facial expressions of pain in the laboratory mouse. *Nat. Methods* **7**, 447–449 (2010). doi:10.1038/nmeth.1455 Medline

55. S. G. Sotocinal, R. E. Sorge, A. Zaloum, A. H. Tuttle, L. J. Martin, J. S. Wieskopf, J. C. Mapplebeck, P. Wei, S. Zhan, S. Zhang, J. J. McDougall, O. D. King, J. S. Mogil, The Rat Grimace Scale: A partially automated method for quantifying pain in the laboratory rat via facial expressions. *Mol. Pain* **7**, 55 (2011). doi:10.1186/1744-8069-7-55 Medline

56. Y. J. Gao, R. R. Ji, Light touch induces ERK activation in superficial dorsal horn neurons after inflammation: Involvement of spinal astrocytes and JNK signaling in touch-evoked central sensitization and mechanical allodynia. *J. Neurochem.* **115**, 505–514 (2010). doi:10.1111/j.1471-4159.2010.06946.x Medline

57. C. Abbadie, Y. Pan, C. T. Drake, G. W. Pasternak, Comparative immunohistochemical distributions of carboxy terminus epitopes from the mu-opioid receptor splice variants MOR-1D, MOR-1 and MOR-1C in the mouse and rat CNS. *Neuroscience* **100**, 141–153 (2000). doi:10.1016/S0306-4522(00)00248-7 Medline

58. L. Y. Liu-Chen, S. X. Li, R. J. Tallarida, Studies on kinetics of [^{3}H]beta-funaltrexamine binding to mu opioid receptor. *Mol. Pharmacol.* **37**, 243–250 (1990). Medline

59. M. D. Aceto, W. L. Dewey, P. S. Portoghese, A. E. Takemori, Effects of beta-funaltrexamine (beta-FNA) on morphine dependence in rats and monkeys. *Eur. J. Pharmacol.* **123**, 387–393 (1986). doi:10.1016/0014-2999(86)90713-2 Medline

60. S. Le Guen, C. Gestreau, J. M. Besson, Morphine withdrawal precipitated by specific mu, delta or kappa opioid receptor antagonists: A c-Fos protein study in the rat central nervous system. *Eur. J. Neurosci.* **17**, 2425–2437 (2003). doi:10.1046/j.1460-9568.2003.02678.x Medline

61. D. E. Gmerek, J. H. Woods, Effects of beta-funaltrexamine in normal and morphine-dependent rhesus monkeys: Observational studies. *J. Pharmacol. Exp. Ther.* **235**, 296–301 (1985). Medline

62. S. Sirohi, S. V. Dighe, P. A. Madia, B. C. Yoburn, The relative potency of inverse opioid agonists and a neutral opioid antagonist in precipitated withdrawal and antagonism of analgesia and toxicity. *J. Pharmacol. Exp. Ther.* **330**, 513–519 (2009). doi:10.1124/jpet.109.152678 Medline

63. L. M. Bohn, R. J. Lefkowitz, R. R. Gainetdinov, K. Peppel, M. G. Caron, F. T. Lin, Enhanced morphine analgesia in mice lacking beta-arrestin 2. *Science* **286**, 2495–2498 (1999). doi:10.1126/science.286.5449.2495 Medline

64. C. Zöllner, S. A. Mousa, O. Fischer, H. L. Rittner, M. Shaqura, A. Brack, M. Shakibaei, W. Binder, F. Urban, C. Stein, M. Schäfer, Chronic morphine use does not induce peripheral

tolerance in a rat model of inflammatory pain. *J. Clin. Invest.* **118**, 1065–1073 (2008). Medline

65. L. M. Bohn, R. R. Gainetdinov, F. T. Lin, R. J. Lefkowitz, M. G. Caron, Mu-opioid receptor desensitization by beta-arrestin-2 determines morphine tolerance but not dependence. *Nature* **408**, 720–723 (2000). doi:10.1038/35047086 Medline

66. F. Noble, S. Turcaud, M. C. Fournié-Zaluski, B. P. Roques, Repeated systemic administration of the mixed inhibitor of enkephalin-degrading enzymes, RB101, does not induce either antinociceptive tolerance or cross-tolerance with morphine. *Eur. J. Pharmacol.* **223**, 83–89 (1992). doi:10.1016/0014-2999(92)90821-K Medline

67. M. S. Buchsbaum, G. C. Davis, W. E. Bunney Jr., Naloxone alters pain perception and somatosensory evoked potentials in normal subjects. *Nature* **270**, 620–622 (1977). doi:10.1038/270620a0 Medline[BPO1]

68. J. D. Levine, N. C. Gordon, H. L. Fields, Naloxone dose dependently produces analgesia and hyperalgesia in postoperative pain. *Nature* **278**, 740–741 (1979). doi:10.1038/278740a0 Medline

69. R. H. Gracely, R. Dubner, P. J. Wolskee, W. R. Deeter, Placebo and naloxone can alter post-surgical pain by separate mechanisms. *Nature* **306**, 264–265 (1983). doi:10.1038/306264a0 Medline

70. J. K. Zubieta, Y. R. Smith, J. A. Bueller, Y. Xu, M. R. Kilbourn, D. M. Jewett, C. R. Meyer, R. A. Koeppe, C. S. Stohler, Regional mu opioid receptor regulation of sensory and affective dimensions of pain. *Science* **293**, 311–315 (2001). doi:10.1126/science.1060952 Medline

71. C. H. Tambeli, J. D. Levine, R. W. Gear, Centralization of noxious stimulus-induced analgesia (NSIA) is related to activity at inhibitory synapses in the spinal cord. *Pain* **143**, 228–232 (2009). doi:10.1016/j.pain.2009.03.005 Medline

72. M. Kaur, A. Liguori, W. Lang, S. R. Rapp, A. B. Fleischer Jr., S. R. Feldman, Induction of withdrawal-like symptoms in a small randomized, controlled trial of opioid blockade in frequent tanners. *J. Am. Acad. Dermatol.* **54**, 709–711 (2006). doi:10.1016/j.jaad.2005.11.1059 Medline

73. B. Chai, W. Guo, F. Wei, R. Dubner, K. Ren, Trigeminal-rostral ventromedial medulla circuitry is involved in orofacial hyperalgesia contralateral to tissue injury. *Mol. Pain* **8**, 78 (2012). doi:10.1186/1744-8069-8-78 Medline

74. D. V. Tillu, G. F. Gebhart, K. A. Sluka, Descending facilitatory pathways from the RVM initiate and maintain bilateral hyperalgesia after muscle insult. *Pain* **136**, 331–339 (2008). doi:10.1016/j.pain.2007.07.011 Medline

75. S. Hatashita, M. Sekiguchi, H. Kobayashi, S. Konno, S. Kikuchi, Contralateral neuropathic pain and neuropathology in dorsal root ganglion and spinal cord following hemilateral nerve injury in rats. *Spine* **33**, 1344–1351 (2008). doi:10.1097/BRS.0b013e3181733188 Medline

76. H. Y. Zhou, S. R. Chen, H. Chen, H. L. Pan, Opioid-induced long-term potentiation in the spinal cord is a presynaptic event. *J. Neurosci.* **30**, 4460–4466 (2010). doi:10.1523/JNEUROSCI.5857-09.2010 Medline

77. A. R. Weyerbacher, Q. Xu, C. Tamasdan, S. J. Shin, C. E. Inturrisi, *N*-Methyl-D-aspartate receptor (NMDAR) independent maintenance of inflammatory pain. *Pain* **148**, 237–246 (2010). doi:10.1016/j.pain.2009.11.003 Medline

78. J. Sandkühler, D. Gruber-Schoffnegger, Hyperalgesia by synaptic long-term potentiation (LTP): An update. *Curr. Opin. Pharmacol.* **12**, 18–27 (2012). doi:10.1016/j.coph.2011.10.018 Medline

79. J. Liauw, L. J. Wu, M. Zhuo, Calcium-stimulated adenylyl cyclases required for long-term potentiation in the anterior cingulate cortex. *J. Neurophysiol.* **94**, 878–882 (2005). doi:10.1152/jn.01205.2004 Medline

80. F. Wei, K. I. Vadakkan, H. Toyoda, L. J. Wu, M. G. Zhao, H. Xu, F. W. Shum, Y. H. Jia, M. Zhuo, Calcium calmodulin-stimulated adenylyl cyclases contribute to activation of extracellular signal-regulated kinase in spinal dorsal horn neurons in adult rats and mice. *J. Neurosci.* **26**, 851–861 (2006). doi:10.1523/JNEUROSCI.3292-05.2006 Medline